Abundance Ratio Trends and Nucleosynthesis in Elliptical Galaxies and Spheroids

Guy Worthey[1]
Department of Physics and Astronomy, St. Ambrose University, Davenport, IA 52803-2829

ABSTRACT

Model and observed spectral feature indices indicate that, in galaxies of all types with velocity dispersions larger than about 225 km s^{-1}, [Mg/Fe] progressively drifts greater than zero, until it reaches $\sim +0.3$ in the largest ellipticals. For elliptical galaxies that have absorption line data for more elements, the abundances of Na and N elevate in a similar fashion, relative to both Ca and Fe ([Ca/Fe] ≈ 0; [Na, N/Fe] progressively > 0). Titanium may also share this apparently generic light-element behavior.

The abundance pattern in elliptical galaxies matches neither the disk, nor the halo, nor the bulge of our own galaxy, although the bulge appears to come the closest. Nitrogen is depleted in the Galactic bulge but elevated in M31, M31's metal rich globular clusters, and large elliptical galaxies. If all measured elements are considered the abundance patterns in our own galaxy and in external galaxies requires the presence of at least three sources of chemical enrichment whose relative contributions can vary from environment to environment. These three sources of enrichment may correspond to Type Ia supernovae (SNs), Type II SNs, and N-rich mass loss from intermediate mass stars, but the behavior of O, Ca, Si, Sc, V, and Ti in the Galactic bulge, disk, and halo seems to require at least one additional supernova flavor.

Abundance ratio effects represent a barrier to the estimation of mean ages from integrated light; a barrier greater than that of isochrone error. Isochrone grids allowing for the variation of individual elements are needed, but relative changes in isochrone temperatures computed as a function of abundance pattern need to be accurate to roughly 7 K if 5% age estimates are desired.

Subject headings: Galaxy: abundances — nuclear reactions, nucleosynthesis, abundances — galaxies: abundances — galaxies: elliptical and lenticular, cD — galaxies: formation — galaxies: stellar content

---

[1]Hubble Fellow

1. Introduction

The observation of variable abundance ratios among the nuclei of galaxies, with most of the data available for elliptical galaxies only, is a useful clue for formation and chemical enrichment history scenarios. This paper synthesizes previous work on Mg and Fe abundances with data on N, Ca, Na, and Ti from the Lick/IDS spectra (Worthey et al. 1994; Trager et al. 1998). This paper serves as a progress report on the present state of knowledge based on the Lick/IDS spectra, but it is not meant as a comprehensive review of current thinking about galaxy formation, chemical evolution, spectral index systems, or models of integrated light. A historical review and a discussion of [Mg/Fe] is presented in the next section, followed by an extension of the discussion to other elements in section 3. The fourth section discusses nucleosynthesis and possible hints for galaxy formation, the fifth details some implications for spectroscopic age determination, and the sixth gives a short summary.

2. Historical Development

Although the *idea* of altered abundance ratios in galaxies must have been considered at least a decade before, the first literature reference discussing altered abundance ratios with any depth appears to be O'Connell (1976) , followed by Peterson (1976), both of whom discussed the strong Na and Mg features (as compared to Fe and Ca features) found in the spectra of elliptical galaxies. O'Connell stated that "our observations also suggest relative abundance variations, although accurate abundances cannot be deduced from synthesis models without a library encompassing a large range of metallicity." Peterson thought that real relative abundance variations were "strongly indicated" and went on to explain how current ideas in nucleosynthesis could account for the overabundance of some species.

However, at that time, the behavior of strong absorption features in the spectra of ellipticals and bulges was usually attributed to an overall metallicity enhancement (Faber 1973), with some authors invoking a substantial contribution of KM dwarf light (Spinrad & Taylor 1969; 1971). O'Connell's and Peterson's papers, though prescient and observationally correct, do not appear to have been influential in the following decade in regard to the issue of relative abundance anomalies. According to Bob O'Connell (private communication), the idea of element ratio changes was discussed in conversation at a subsequent conference stellar populations at Yale University (proceedings: Tinsley & Larson 1977) but was rejected as unlikely; it was thought that "normal" element enrichment above the solar value would probably produce the spectral changes seen. The issue of variable abundance ratios was not discussed in the proceedings of the conference.

A substantial time gap intervened before Worthey, Faber, & González (1992, hereafter WFG) discussed absorption line strengths again (this time Mg and Fe features) and came to the same conclusion as O'Connell (1976) and Peterson (1976): Mg abundance is enhanced compared to Fe in large ellipticals. See also Peletier (1989) and Faber, Worthey & González (1992). WFG's argument was stronger because their modelling effort included spectra from local stars of high metallicity, so that a "normal" abundance increase was shown not to be a viable option. By 1992 the pattern of variable abundance ratios in *stars* as a function of abundance was well established (e.g. Wheeler, Sneden, & Truran 1989) and these observations were explained by two varieties of supernova enrichment; type I and type II supernovae. This readily explains how [Mg/Fe] *could* be made to vary, and the idea that [Mg/Fe] *did* vary among elliptical galaxies was accepted. Subsequent work has concentrated on model calibrations and attempts to include variable [Mg/Fe] in the models (Weiss, Peletier, & Matteucci 1995; Barbuy 1994; Borges et al. 1995; Bressan, Chiosi, & Tantalo 1996).

Instead of optimizing the addition of stellar spectra to match galaxy spectra (like Faber 1972; O'Connell 1976; Pickles 1985), these later efforts use isochrone-based models. The isochrones and an assumed initial mass function (IMF) give the numbers and luminosities of the stars present as a function of (assumed scaled-solar) abundance and population age. With some prescription for star colors or star spectrophotometry, monochromatic fluxes can be computed for each model star, and thus integrated colors can be computed. Information on spectral indices is summarized separately in fitting formulae that give index strength as a function of stellar parameters. These formulae are used to predict an index strength for each star in the isochrone, and the final integrated index strength is computed as an average, weighted by monochromatic luminosity and number of stars present.

Figure 1 is a reprise of the figures found in WFG that show the [Mg/Fe] drift among galaxies, with data and model updates. Model sequences are shown, always for [Fe/H] $= -0.25$, 0.0, and 0.25, but for different ages, methods, and authors, as explained in the caption. The point about the models is they are multi-degenerate in their locus on the $<$Fe$>$-Mg diagram; always landing roughly at the same locus regardless of age, author, fitting function version, underlying isochrones, flux library, or sophistication of modelling effort. Models add approximately as vectors, so that combinations of ages or metallicities also lie on the same locus. The galaxies show spread far beyond any possible stretch of the models, in the sense that the largest galaxies (solid symbols) have much stronger Mg line strength at a given Fe strength than expected. Since any reasonable combination of local stars will fail to fit the galaxies, the conclusion is reached that a real Mg overabundance exists in large Es.

It is important to realize that whatever abundance trends are present in the calibrating stars are frozen into the index fitting functions. For example, model index strengths match globular cluster integrated index strengths even though globular cluster giants clearly have [Mg/Fe] at least a factor of 2 above solar. This is because globular cluster giants were used for the calibration. There is therefore potential danger at metallicities near solar and above if the calibrating stars have abundance ratio drifts. High quality, high resolution spectroscopy data of stars more metal rich than the sun (McWilliam 1990; Edvardsson et al. 1993; Luck & Challener 1995) seem to indicate that the light elements are near the solar ratio. We therefore feel *mostly* comfortable with saying "[Mg/Fe] is greater than zero in large Es" rather than the more precise "[Mg/Fe] in large Es is greater than that of local metal rich stars," but there remains much observational work on local stars before we can be certain.

The magnitude of the [Mg/Fe] overabundance is around 0.3 dex or a little greater for the largest Es (WFG, Weiss et al. 1995, Borges et al. 1995). Precise absolute measurements of [Mg/Fe] are tricky, but relative trends in [Mg/Fe] can be measured almost to the accuracy of the observations, roughly 0.1 dex for Lick/IDS data, 0.05 dex for González $R_e/8$ data for individual galaxies.

Gradients within elliptical galaxies in Fe and Mg indices (Fig. 1; WFG; Davies, Sadler, & Peletier 1993; Carollo & Danziger 1994; Fisher, Franx, & Illingworth 1995) are "steeper than the relationship linking galaxy nuclei" with a few exceptional galaxies. When the models are superimposed on the data it appears that [Mg/Fe]$\approx$constant within a galaxy, even though the overall [Mg/Fe] varies from galaxy to galaxy.

Some [Mg/Fe] information is available on spiral bulges. Sil'chenko (1993) finds that [Mg/Fe] is solar in most bulges of other spiral galaxies, even though it is enhanced in Es and our own Galactic bulge (McWilliam & Rich 1994). Jablonka, Martin, & Arimoto (1996) find that very luminous bulges show enhanced [Mg/Fe] but fainter ones do not, similar to Es. The situation among S0 galaxies is author-dependent at the moment (Sil'chenko 1993 versus Fisher, Franx, & Illingworth 1996), but the Sil'chenko sample of disk galaxies contains very few galaxies with Mg_2 greater than about 0.3, implying that only galaxies of modest or low velocity dispersion are in the sample (because of the observed tight correlation between velocity dispersion and Mg line strength; e.g. Bender, Burstein, & Faber 1993.) In sum, the data available to date seem to indicate that [Mg/Fe] is near zero in most galaxies of *all* types with velocity dispersion less than about 225 km s^{-1}, but galaxies with velocity dispersions above that value are progressively more Mg-enhanced. This type-independence is a new conclusion.

We defer discussion of the implications of [Mg/Fe] drift to section 4, first discussing the other elements for which data is available.

3. Elements N, Na, Mg, and Ti

The spectrum of any large, dynamically hot galaxy can be viewed only at resolutions appropriate to the velocity dispersion of the individual stars within it due to the smearing effect of the combined stellar doppler shifts. This resolution is on the order of 10 Å (at ∼5000Å) for the largest galaxies. Such a resolution swamps many weak features and makes even strong features blend with neighbors and it can be readily seen that the clean separation of individual transitions enjoyed by high resolution stellar spectroscopists is unattainable in large galaxies. Some clean features persist nevertheless (Mg b and Na D are the most obvious) and others are only modestly blended so that a good deal of information on individual species can be extracted.

The data and models are on the "Lick/IDS" system (Burstein et al. 1984, Worthey et al. 1994). These star and galaxy data were collected at Lick Observatory from 1972 to 1984 with the same telescope, instrument, and IDS detector. In the Lick index scheme, flanking "pseudocontinuum passbands" are defined to either side of the absorption feature of interest. The average fluxes in these bands are found, and a straight line is drawn from midpoint to midpoint that represents the pseudocontinuum. The missing flux in the "index passband" is integrated and expressed as either an equivalent width in Å or a flux ratio in magnitudes. Each index is measured in a large collection of stars that cover the metallicity range in addition to gravity and temperature. Index behavior is summarized by polynomial fitting functions (Worthey et al. 1994) and incorporated into isochrone-based population models (Worthey 1994). For convenience we use these models, but the conclusions are robust against variations in author, as was the case for [Mg/Fe] in the introduction.

The indices are summarized in Table 1, a version of which first appeared in Worthey (1996). The indices are those of Worthey et al. (1994) except for those Hγ and Hδ indices marked "WO97," which are described in Worthey & Ottaviani (1997). The indices are grouped into 10 families according to what species they measure. The information on what species are present comes largely from the theoretical work of Tripicco & Bell (1995). Parentheses in the "other species" column indicate that addition of that element contributes negatively to that index. Worthey & Ottaviani (1997) indices have yet to be assayed for abundance ratio sensitivity. The column of "metal sensitivities" are partial derivatives of the Worthey (1994) population models (d log age / d log Z at constant index) giving the relative sensitivity of the index to metallicity compared to its sensitivity to age. These numbers will be important in the section after the next.

As outlined in the introduction, the evidence for non-solar abundance ratios comes from the mismatch between scaled-solar population models and galaxies (Fig. 2). Many index-index pairs are very well reproduced by the models. For instance, in all intercomparisons of Table 1 families 2, 4, and 5 the models fall on top of the galaxies; see Worthey (1994) for illustrations. In WFG, the Mg_2, <Fe> pair was singled out because the features are immediately adjacent, thus eliminating any possible wavelength dependence of the models. As our confidence in the basic correctness of the models grows, additional features can be highlighted. Worthey (1996) showed Na, CN, and Ca plots like those in Figure 2. In all the diagrams, composite subpopulations add approximately as vectors, but since all age-metallicity combinations are located along the same trajectory they cannot induce off-trajectory changes.

Figure 2 tells us that Na and N behave in a way exactly similar to Mg with respect to Fe: a systematic enhancement exists for the larger galaxies, but not the small ones. In the case of CN, we can pinpoint N rather than C because the CN-strongest galaxies are *not* strong in the G band (CH) or Fe4668 (C_2) indices. We would expect this in any case since N is the least abundant of the elements C, N, and O, and the interplay of these three elements in cool stars is such that extra C is readily incorporated into CO molecules, but extra N makes more CN molecules (e.g. Tripicco & Bell 1995). Indices Ca4455 (shown) and Ca4227 (not shown) overlay the models, in accord with O'Connell's (1976) observation that Ca H and K strength is consistent with Fe feature strength.

The TiO_1 and TiO_2 plots in Fig. 2 were not shown in Worthey (1996). They illustrate problems that lie mostly with the models. Most modeled indices are very insensitive to the underlying evolutionary isochrones (e.g. Fig. 1), but not TiO. The TiO index is strong only in late K and M giants and is very sensitive to the luminosity function and especially the temperature structure of the high luminosity tip of the RGB. The modest upper RGB temperature differences between the Worthey (1994) and Padova (Bertelli et al. 1994) isochrone sets are enough to render model TiO unreliable and any absolute [Ti/Fe] measurement impossible. This particular model defect has not been highlighted in previous literature.

Despite this defect, we notice that the model trajectories are firmly vertical, whatever model variety is used. In contrast to this vertical prediction, there is a distinct horizontal segregation of high-σ and low-σ galaxies. We therefore deem it probable that there is some systematic variation in [Ti/Fe] with galaxy size, with larger galaxies having more TiO absorption. It is not possible to measure the overabundance with current models. This is a new conclusion.

In contrast to TiO versus Fe we note that the diagram of TiO_1 versus TiO_2 is degenerate with respect to upper RGB temperature because the temperature dependences of the two TiO indices are very similar. This diagram was shown in Worthey (1994). In it, the galaxies still do not follow the model line, and Worthey (1994) concluded on the basis of the spectrum of β Peg, an M2 giant (Davis 1947), that [V + Sc / Ti] may be varying among galaxies. We have no new evidence to apply to this observation.

4. Nucleosynthesis and galaxy formation

The previous sections synthesize from previous refereed (WFG; Worthey 1994) articles and conference proceedings (Worthey 1996). It was found that Mg, Na, and N are globally enhanced in large Es, but nearly local-disk-like in small ones. Ca seems lockstep with Fe, and there is a chance that [Sc + V / Ti] is variable. New conclusions are that the Mg enhancement applies to galaxies of every type, starting at $\sigma \approx 225$ km s^{-1}, and that [Ti/Fe] probably follows the generic light element behavior, with caveats regarding uncertain models and larger data errors. We now discuss these trends with respect to nucleosynthetic theory and observations of local abundance trends.

Several processes can explain an overall light element enhancement as a function of galaxy size (Worthey 1992). Most schemes vary the ratio of the number of Type II vs. Type Ia supernovae (SNs) that contribute to the chemical enrichment of small versus large galaxies. Type II SNs contribute light elements plus Fe, while Type I SNs contribute almost all Fe-peak elements. Type I SNs are usually assumed to come from binary accretion on to white dwarfs, and are generally thought not to result from stars more massive than 5 to 10 $M_\odot$. Because of this, there is a time delay of a few times 10^8 years from initial star formation and the release of Fe-peak ejecta from Type I SNs.

Although there are several possibilities for varying the ratio of the two types of SNs as a function of galaxy size, including binarism and creative wind scenarios, the two taken most seriously are (1) formation timescale, which, if shorter in large galaxies, can lead to more light element enrichment before Type I enrichment has a chance to contribute, and (2) an IMF variation keyed to environment such that a larger velocity dispersion leads to more massive stars being produced. This will also enhance light elements in larger galaxies.

The first scenario predicts good correlation of Mg strength with dynamical crossing time, or, in the case of termination of star formation by supernova winds (e.g. Arimoto & Yoshii 1987), with potential depth, and the second would predict good correlation with σ. In fact, the Mg$_2$ versus σ correlation is famous for its tightness, while the <Fe> versus σ correlation is virtually nil, suggesting a tight link between Mg abundance and velocity dispersion. This is strengthened by the new conclusion that galaxy type does not matter in the [Mg/Fe] versus velocity dispersion diagram. The Na D and CN indices also correlate tightly with σ. According to chemical evolution models (Matteucci & Padovani 1993) the required change in IMF slope to effect a 0.3 dex change in light element abundance is not large (a power-law slope change of 0.4 is more than sufficient). Another discriminant between the two scenarios is the content of the interstellar gas. In the timescale scenario, Fe-rich gas is expelled soon after star formation, but in the IMF scenario Fe is truly deficient compared to the lighter Type 2 ejecta. X-ray spectra (Loewenstein & Mushotzky 1996) seem to show that Mg and Si are enhanced compared to Fe, supporting the IMF scenario. However, if the suspiciously low overall IGM metallicity inferred from X-ray observations is due to difficulties in modelling the Fe atom the evidence will have to be reconsidered.

We now go on to discuss E and spheroid abundance ratios within the framework of empirical Galactic data for stars of different abundance and current nucleosynthetic wisdom, extending the discussion of Worthey (1996). The nucleosynthetic picture to which we refer is essentially that effectively summarized by Woosley & Weaver (1995, hereafter WW95).

4.1. C, N, O

In Figure 3 we plot observed halo, disk, and bulge abundance ratios as a function of [Fe/H] in a smoothed manner, where stellar data has been taken mainly from Timmes, Woosley, & Weaver (1995) and references therein, and McWilliam & Rich (1994, hereafter MR94). In the halo and disk, N and C are almost solar. MR94 did not look at N or C, but Rich (1988) and Terndrup & Sadler (1996) find that bulge K giants have systematically *weak* CN. With [O/Fe]≈0, this means that N is underabundant in the bulge. Elliptical galaxies and M31, on the other hand, clearly have enhanced N. Nitrogen itself is thought to come from mass-loss from intermediate and low mass stars (WW95), and presumably some modulation of this mechanism causes N to vary so strongly from environment to environment. We revisit N below.

Oxygen is an unknown in ellipticals at present, but it could probably be measured via appropriately thorough stellar calibration work on the 2.3μ CO feature or perhaps other molecular features involving O. The low [O/Fe] found by MR94 in the bulge at [Fe/H] $= -1$ is a surprise since Mg and most other "alpha" elements are enhanced, and O is thought to be co-produced with the alphas in Type II nucleosynthesis (WW95). The low O abundance is not consistent with the current picture of nucleosynthesis. MR94 also note that the low-abundance halo Ca and Si ratios do not extrapolate to higher abundance, and this is also a problem if the bulge is thought to be enriched by primarily Type II ejecta.

4.2. Mg, Ca, Na

Ca tracks Fe with a trajectory such that [Ca/Fe] is high in the halo and low-abundance bulge stars, but near zero in the solar neighborhood. Since Ca in elliptical galaxies follows Fe exactly, apparently the behavior of Ca with Fe is the same in all Galactic and extragalactic environments. Nucleosynthesis theory (WW95) predicts that the abundant isotope of Ca comes primarily from explosive and normal Oxygen burning and follows the observed halo and disk [Ca/Fe] trend quite well (Timmes et al. 1995). If Type I enrichment is not allowed in the bulge, the fact that [Ca/Fe] abundance is low in the bulge at [Fe/H]=0 means that either the Ca yield of Type II supernovae modulates with metallicity or that there are at least two "flavors" of Type II enrichers. Neither of these two possibilities is theoretically predicted.

Produced by quiescent C and Ne burning, Mg is enhanced in the halo (Wheeler et al. 1989), in the bulge (MR94), and in large elliptical galaxies, but normal in the disk and in the bulges of medium-sized and smaller spirals (WFG, Jablonka et al. 1996). These observations are readily explained by a Type II / Type I enrichment variation in which halo, bulge, and large Es have more Type II enrichment. A possible exception to this is the Galactic bulge. Its enhanced [Mg/Fe] despite its modest velocity dispersion (MR94) may be a puzzle.

Sodium is produced in nearly the same nucleosynthetic environment as Mg, and theoretically should have a similar abundance behavior. Roughly, it does, being enhanced in large Es and also in the Galactic bulge. The bulge Na abundance is uncertain at the present time due to difficulties in using the Na D lines for abundance work (MR94).

4.3. Sc, V, Ti

Elements Sc, V, (odd atomic number) and Ti (even atomic number) are made primarily during explosive nucleosynthesis and hence are sensitive to many uncertainties in theoretical prediction of the yields (WW95). Regardless of this, the Galactic pattern shows Sc and V tracking Fe in all environments except the bulge, where they are high. Titanium is high in the halo, low in the disk, and high in the bulge. In a straightforward picture in which a Type II "alpha" mixture is diluted by Type I Fe-peak elements in the disk *alone* the trio Sc, V, and Ti is a puzzle. In Es, a TiO_2 versus velocity dispersion plot resembles a light-element tight correlation more than a Fe-peak scatter plot. If the TiO_2 index is in fact sensitive to Sc + V, then the Sc + V pattern is more reminiscent of alpha element behavior, with Ti as measured by TiO_1 following the behavior of iron. An alternative explanation is that TiO_1

does *not* measure Ti, but other Fe-peak elements. In that case, TiO_2 may faithfully follow Ti abundance and we would conclude that Ti behaves like a generic light element and that we can make no conclusion about Sc + V.

We are driven to conclude that either the data is misleading, or nature is rich in complexity. The halo pattern (Ti up, Sc, V down), the disk pattern (Ti, Sc, V down), the bulge pattern (Ti, Sc, V up), and the pattern in large ellipticals (Ti probably up, Sc + V inconclusive) force the inclusion of at least two nucleosynthetic variables. That is, Type I/Type II ratio is one variable, easily responsible for the disk-bulge difference, but unable to explain how the distinct halo pattern can transform into *both* the disk and the bulge pattern. Thus, at least one additional SN flavor appears to be required.

Titanium is a difficult element for theoretical prediction, with one isotope falling at least a factor of 6 short of matching the observed disk abundance (Timmes et al. 1995). Scandium and V are also underproduced, but not as badly. Titanium is coproduced with Fe in explosive nucleosynthesis; Sc and V are created in the "alpha-rich freeze-out" in the very deepest of expelled layers (WW95).

4.4. Chemical Evolution and Nucleosynthesis

Looking over all the patterns in Figure 3, one thing to note is that extrapolation of the halo abundance pattern to higher overall Z is not sufficient to mimic either the bulge or Es. Wrong answers will be obtained for N, Na, and Ca for sure, probably O, Ti, Sc, and V. This will have impact on age determination, as explained in the next section. The Galactic bulge may provide a much better abundance pattern template for Es, but N is anomalous. It is not yet clear whether Na matches or not.

The different abundance ratios in different environments must be linked to different kinds of supernova or other enrichment mechanisms. A lower limit on the number of enrichment mechanisms can be placed empirically by pretending ignorance of the theoretical Type II, Type I picture. Any enrichment mechanism could, in principle, have an abundance pattern that shifts with overall metallicity. Since there are many instances in Figure 3 where different ratios exist at the same [Fe/H], there must be at least two sources of enrichment in operation. If we consider the Ti, V, Sc trio of three paragraphs ago we need three sources of enrichment. This total jumps to four when we consider N in the bulges of M31 and the Milky Way because the abundance ratios in those two places seem identical *except* for N, which is clearly much more abundant in M31. Discounting the { Sc, V, Ti } evidence for the moment, at least 3 sources of chemical enrichment are required. This is a new conclusion.

Tentatively, we can assign the three sources of enrichment to the currently accepted culprits: (1) Type II supernovae for light metals, primary N, and some Fe as well, (2) Type Ia supernovae for Fe-peak elements, and (3) CNO nucleosynthesis in intermediate mass stars for secondary N. When we do this assignation, we must realize that the low bulge O, Ca, and Si abundances are *not* predicted by current theoretical Type II yield estimates for stars of various masses (WW95), and the Ti, V, Sc trio presents a similar problem. Resolving these inconsistencies would seem to involve revising supernova yields and probably allowing for more than one kind of Type II SN enricher.

The Milky Way-M31 nitrogen dichotomy is even more interesting when one considers M31's globular clusters. Indices <Fe> and CN_1 are shown in Figure 4 for Galactic and M31 globular clusters and galaxies. Due to lack of calibration stars, model CN_1 strength is uncertain at low metallicity, but in the reliable range the whole globular cluster sequence looks substantially N-rich, joining with the large Es at the upper end of the sequence. But unlike the galaxies, the metal-rich globular clusters do not have excess Mg or Na: the models lie on top of the <Fe>, Mg_2 or NaD sequences as seen, for instance, in Burstein et al. (1984). This causes the M31 globular clusters to dramatically separate from the galaxies in the Mg_2-CN_1 diagram, also shown in Burstein et al. (1984).

The metal-rich M31 globular clusters are spatially spread out over the whole M31 halo, over the same area that the metal-poor clusters occupy (van den Bergh 1962), but with metallicities 10 to 100 times higher. This spatial distribution appears somewhat similar to that found in at least some globular cluster systems of large Es: some metal-rich clusters are found at large radius, but they become much more numerous relative to metal-poor clusters at small radius (Geisler, Lee, & Kim 1996). The M31 clusters generally have a *Galactic disk* abundance distribution where all indices follow the models closely except for the CN indices. In terms of a Type II, Type I picture, the metal-rich M31 globular clusters must have substantial Type I enrichment because they are Fe rich. There must also have been a substantial extra supply of Nitrogen. And the enrichment that occurred happened over a 20 to 30 Kpc radius!

The contrast between the Milky Way and M31 is extreme. The Milky Way bulge has $[N/Fe] < 0$, M31 has $[N/Fe] > 0$, with an abundance difference at least a factor of two, more likely a factor of 5 or greater. Magnesium abundance is almost in the solar ratio in M31, but elevated in the Milky Way's bulge. The Milky Way has no metal rich $[Fe/H] > -0.5$ globular clusters except very near its nucleus while M31 has metal rich clusters that are cospatial with its metal poor clusters tens of Kpc away from the galaxy's center. M31 must therefore have had a much different chemo-dynamical history than the Milky Way, with some sort of Fe-rich, N-very-rich galactic wind episode that enriched an enormous volume of space, with subsequent globular cluster formation from this enriched material.

The source of the extra N in M31 is an open conjecture. One guess is that there was a massive episode of star formation in which stars more massive than around 10 $M_{\odot}$ were relatively rare. Perhaps this episode was the second major episode of star formation so that a pool of Fe-peak elements from Type I supernova was already available. An excess of N could be built up from an excess of intermediate-mass stars, and whatever Fe is available from past or present Type I supernovae would be preserved without overwhelming competition from Type II enrichment. This would have to be followed by an energetic supernova wind phase that blew at least some enriched clouds far into the halo where they formed Fe-rich, N-rich globular clusters.

5. Spectroscopic Age Determination

We now go on to discuss direct spectroscopic age determinations in light of changing element ratios. This discussion follows Worthey (1996; 1997) conference proceedings articles. It is difficult to quantitatively specify the star formation history of an E even in two-bin histograms of "old" or "young" stars due to the complication of metallicity and its nearly overwhelming similarity to age effects if the percentage change in age/Z is $-3/2$ (Aaronson et al. 1978; Worthey 1994). However, in the "sensitivity" column of Table 1, notice that compared to metal-sensitive indices like Fe4668, the Balmer features are relatively metal-insensitive, or age-sensitive, thus opening the possibility that some metal-Balmer index pairs can break the otherwise omnipresent age-metal degeneracy. In the Balmer-metal diagrams shown in Figure 5, the models do indeed occupy a *region* rather than a *locus*, and the galaxies tend to fill the region.

Despite several scholarly attempts to calibrate the measurement errors in Lick/IDS data, the errors remain incompletely established. The present error estimates are based on a Fourier measurement of the channel-to-channel noise due to Poisson statistics, and we expect (but cannot yet prove) that these errors are good to $\pm 20\%$. If the current errors are of this quality, then we can make the following conclusions from the age-diagnostic Balmer-metal diagrams such as those shown in Figure 5. First, real scatter in mean age exists, where "mean age" is the light-weighted sum of the ages of the stellar populations present. Operationally, the mean age is the age that one infers from a Balmer-metal diagram. Second, the scatter in age is larger in the smaller galaxies. Notice how the solid symbols (large galaxies) tend to clump more stongly than the empty (smaller galaxies) symbols.

The third point *would be* to make a statement about the overall mean ages of the galaxies based on their location in the model grid. However, in the top panels of Fig. 5, notice how the median galaxy drifts from panel to panel. Versus <Fe>, the galaxies look as old as the universe and just under solar metallicity. Versus Mg_2, the galaxies appear a lot more metal rich than the model grid can cover (maybe +1.0 dex) and about 2 Gyr old. Versus Fe4668, the ages and metallicities come out to be about the same as the geometric mean of <Fe> and Mg_2. This large range (a factor of 10!) in age estimates is caused by abundance ratio effects. Mg strength is anomalously great compared to Fe strength, especially in large galaxies, seriously skewing the <Fe>- and Mg_2-based age estimates because of the residual interdependency of age and metallicity. Going to a more sensitive metallicity indicator like Fe4668 helps significantly, but only in the case of an idealized index combination that measures age and metallicity in a completely orthogonal way can an age estimate be isolated from metallicity effects.

However, even ideal age indices will not give the correct age if abundance ratios are varying. Nearly ideal indices that appear to measure *only* age (e.g. the $H\gamma_{HR}$ index; Jones & Worthey 1995) can be found. These indices cleanly measure the difference in temperature between the main sequence turnoff and the RGB, but this temperature difference can be modulated by abundance ratio changes. Stellar evolution modeling of different composition mixtures shows that Oxygen abundance has this effect (Fig. 6; VandenBerg 1992; Straniero, Chieffi, & Salaris 1992), and helium might also (Weiss et al. 1995). A systematic exploration of temperature effects from abundance ratio changes has not been attempted, especially not for metal-rich populations.

Fundamentally, spectroscopic age indicators will always measure the temperature difference between the turnoff and giant branch. The key question is can abundance ratio differences produce enough of a temperature shift to be important. Using the population models, we note that a global shift of the whole isochrone by 100 K leads to an age estimate that is off by about 70%. Scaling this rough number, if we want ages accurate to 5% we need isochrones accurate to 7 K. This rough estimate should provide a benchmark for deciding whether candidate opacity sources are significant or not when calculating stellar structure. Figure 6 shows the enormous effect that a factor of 4 oxygen overabundance has on turnoff temperature (about 100 K) without affecting the RGB temperature at all. It seems plausible that other relatively abundant elements will have effects severe enough to significantly skew age estimates if their abundance varies.

To summarize, the uncertainty in mean age from abundance ratios comes from two sources; the straightforward effect of spectral changes due to altered abundances in the photospheres of stars, and the second order effect of altered stellar evolutionary timescales, luminosities, and (especially) temperatures. Both effects are serious and both require comprehensive theoretical modeling efforts to quantify well. Blind application of current models gives wildly different age estimates depending on the Balmer-metal diagram, and the scatter from this is much greater than the ∼35% uncertainty due to errors in model-building (Charlot, Worthey, & Bressan 1996). A substantive effort in this regard promises to provide reliable and meaningful mean ages for nearby and distant dormant galaxies.

6. Summary

- In large elliptical galaxies and spheroids the abundances of Mg, Na, and N are elevated compared to a scaled-solar mixture, while Ca and Fe are not. The enhancements are mild, reaching a few tenths of dex for the largest galaxies.
- It is likely that Ti also follows this light-element pattern.
- In the case of Mg, enough data exist to say that the trend of [Mg/Fe] with velocity dispersion is independent of galaxy type, with substantial enhancement beginning for galaxies with velocity dispersions greater than about 225 km s^{-1}.
- Worthey's (1994) TiO_1, TiO_2 diagram indicates a possible variation of (V + Sc)/Ti.
- Comparison of the abundance ratio trajectories in the Galactic disk, halo, and bulge with the new galaxian data is a cornucopia of information. Current Type II versus Type I nucleosynthesis models do not correctly predict the low O, Ca, and Si abundances found in the bulge by MR94, which is otherwise matched approximately by the pure Type II mixture predicted by theory.
- The behaviors of either N or the {V, Sc, Ti} trio indicate that at least 3 chemical enrichment sources are required to produce the abundance pattern seen in different environments. The behavior of V, Sc, and Ti seem to indicate that more than one kind of Type II supernova is chemically important, while the behavior of N fingers some mechanism for substantially modulating the amount of N contributed by the intermediate mass stars that are thought to be the dominant N contributor. [N/Fe] is low in the Galactic bulge, zero in the disk and halo, but high in large Es, the nucleus of M31, and M31's metal rich globular clusters.
- M31 has experienced a nucleosynthetic history quite different from that of the Milky Way. (1) M31 has substantially more N in its center, (2) M31 has a metal-rich population of globular clusters that have scaled-solar Fe, Mg, and Na, but are significantly enhanced in N, (3) M31's metal-rich globulars are cospatial with its

metal-poor globular clusters. These points suggest a double-formation scenario involving massive N production followed by a SN wind. This conclusion echos that of van den Bergh (1962).

- Mean age and mean metallicity can be determined from pairs of indices that have different relative age-metal sensitivities. However, abundance ratio effects (1) cause shifts in the metallic indices that then cause age shifts, and (2) abundance ratio changes can cause changes in isochrone temperature structure that can mimic an age effect.

- Even with these problems in mind, among Es and S0s mean age scatter is judged to be real, and the age scatter is larger in smaller galaxies. The age zero point can not yet be addressed from the models alone.

- New isochrone grids are needed that self-consistently model abundance ratio changes. Relative temperature changes need to be accurate to roughly 7 K if 5% age estimates are desired.

This research was funded by NASA through grant HF-1066.01-94A from the Space Telescope Science Institute, which is operated by the Association of Universities for Research in Astronomy, Inc., under NASA contract NAS5-26555. The author would like to thank D. Terndrup for early access to the Galactic bulge star spectral data and M. Tripicco and R. W. O'Connell for insightful conversation.

REFERENCES

Aaronson, M., Cohen, J. G., Mould, J. R., & Malkan, M. 1978, ApJ, 223, 824

Arimoto, N., & Yoshii, Y. 1987, A&A, 173, 23

Barbuy, B. 1994, ApJ, 430, 218

Bender, R., Burstein, D., & Faber, S. M. 1993, ApJ, 411, 153

Bertelli, G., Bressan, A., Chiosi, C., Fagotto, F., & Nasi, E. 1994, A&AS, 106, 275

Borges, A. C., Idiart, T. P., de Freitas Pacheco, J. A., Thévenin, F. 1995, AJ, 110, 2408

Bressan, A., Chiosi, C., & Tantalo, R. 1996, A&A, 311, 425

Burstein, D., Faber, S. M., Gaskell, C. M., & Krumm, N. 1984, ApJ, 287, 586

Charlot, S., Worthey, G., & Bressan, A. 1996, ApJ, 457, 625

Carollo, C. M., & Danziger, I. J. 1994, MNRAS, 270, 523

Davies, R. L., Sadler, E. M., & Peletier, R. F. 1993, MNRAS, 262, 650

Davis, D. N. 1947, ApJ, 106, 28

Edvardsson, B., Andersen, J., Gustafsson, B., Lambert, D. L., Nissen, P. E., & Tomkin, J. 1993, A&A, 275, 101

Faber, S. M. 1972, A&A, 20, 361

Faber, S. M. 1973, ApJ, 179, 731

Faber, S. M., Worthey, G., & González, J. J. 1992, in The Stellar Populations of Galaxies, ed. B. Barbuy & A. Renzini, IAU Symp. 149, 255

Fisher, D., Franx, M., & Illingworth, G. D. 1995, ApJ, 448, 119

Fisher, D., Franx, M., & Illingworth, G. D. 1996, ApJ, in press

Geisler, D., Lee, M. G., Kim, E. 1996, AJ, 111, 1529

González, J. J., 1993, Ph.D. Thesis, Univ. California, Santa Cruz

Jablonka, P., Martin, P., & Arimoto, N. 1996, AJ, 112, 1415

Jones, L. A., & Worthey, G. 1995, ApJ, 446, L31

Loewenstein, M. & Mushotzky, R. F. 1996, ApJ, 466, 695

Luck, R. E., & Challener, S. L. 1995, AJ, 110, 2968

Matteucci, F., & Padovani, P. 1993, ApJ, 419, 485

McWilliam, A. 1990, ApJS, 74, 1075

Table 1: Lick/IDS index families

		dom.	other species	sensitivity	
1.	CN_1	CN	C, N, (O)	1.9	
	CN_2	CN	C, N, (O)	2.1	
2.	Ca4227	Ca	(C)	1.5	weak
3.	G 4300	CH	(O)	1.0	
4.	Fe4383	Fe	C, (Si)	1.9	
	Fe5270	Fe	C, (Mg), Ca	2.3	
	Fe5335	Fe	(C), (Mg), Cr	2.8	
	Fe5406	Fe	(Mg), Cr, C	2.5	
5.	Ca4455	mix	Cr, Ca, Fe, Ni	2.0	
	Fe4531	Ti	Cr, Fe, (Si)	1.9	small range
	Fe5015	mix	Ti, (Mg), Fe	4.0	O III in sideband
	Fe5709	mix	(C), Fe, Ti, Cr	6.5	weak
	Fe5782	Cr		5.1	weak
6.	Fe4668	C_2	(O), (Si)	4.9	
7.	Mg_1	C	Mg	1.8	
	Mg_2	Mg	C	1.8	
	Mg b	Mg	(C)	1.7	
8.	Na D	Na	C	2.1	interstellar extinction
9.	TiO_1	TiO	Ti, (Fe)	1.5	
	TiO_2	TiO	V, Sc, Ti	2.5	
10.	$H\delta_A$	H		0.9	WO97
	$H\delta_F$	H		1.1	WO97
	$H\gamma_A$	H		1.0	WO97
	$H\gamma_F$	H		1.2	WO97
	$H\beta$	H	(Mg), (Cr), C	0.6	

McWilliam, A., & Rich, R. M. 1994, ApJS, 91, 749, MR94

O'Connell, R. W. 1976, ApJ, 206, 370

Peletier, R. F. 1989, Ph. D. Thesis, Univ. of Groningen

Peterson, R. C. 1976, ApJ, 210, L123

Pickles, A. J. 1985, ApJ, 296, 340

Rich, R. M. 1988, AJ, 95, 828

Sil'chenko, O. K. 1993, Pis'ma v Astronomicheskij Zhurnal, 19, 701

Spinrad, H. & Taylor, B.J. 1969, ApJ, 157, 1279

———, 1971, ApJS, 22, 445

Straniero, O., Chieffi, A., & Salaris, M., 1992, Memoirs of the Astronomical Society of Italy, 63, 43

Terndrup, D. M., & Sadler, E. M., 1996, AJ, 112, 171

Timmes, F. X., Woosley, S. E., & Weaver, T. A. 1995, ApJS, 98, 617

Tinsley, B. M., & Larson, R. B., ed., 1977, The Evolution of Galaxies and Stellar Populations (Yale University Obs., New Haven)

Trager, S. C., Worthey, G., Faber, S. M., Burstein, D., & González, J. J. 1998, ApJS, 117, in press (May 1998)

Tripicco, M. J., & Bell, R. A. 1995, AJ, 110, 3035

van den Bergh, S. 1962, AJ, 67, 486

VandenBerg, D. A. 1992, ApJ, 391, 685

Weiss, A., Peletier, R. F., & Matteucci, F. 1995, A&A, 296, 73

Wheeler, J. C., Sneden, C., & Truran, J. W., Jr. 1989, ARA&A, 27, 279

Woosley, S. E., & Weaver, T. A. 1995, ApJS, 101, 181, WW95

Worthey, G., 1992, Ph.D. Thesis, Univ. California, Santa Cruz

———, 1994, ApJS, 95, 107

Worthey, G., Faber. S.M., & González, J. J. 1992, ApJ, 398, 69, WFG

Worthey, G., Faber, S.M., González, J. J., & Burstein, D. 1994, ApJS, 94, 687

Worthey, G. & Ottaviani, D. L. 1997, ApJS, 111, 377

Worthey, G., Trager, S. C., & Faber, S. M. 1996, in Fresh Views on Elliptical Galaxies, ASP Conference Series No. 86, (San Francisco,ASP), ed. A. Buzzoni, A. Renzini, & A. Serrano

Worthey, G. 1997, in From Stars to Galaxies: The Impact of Stellar Physics on Galaxy Evolution, ed. C. Leitherer, U. Fritze-von Alvensleben, & J. Huchra (ASP Conf. Series 98: ASP: San Francisco), 467

Worthey, G. 1997, in Star Formation Near and Far, ed. S. S. Holt & L. G. Mundy (AIP Press: Woodbury), 525

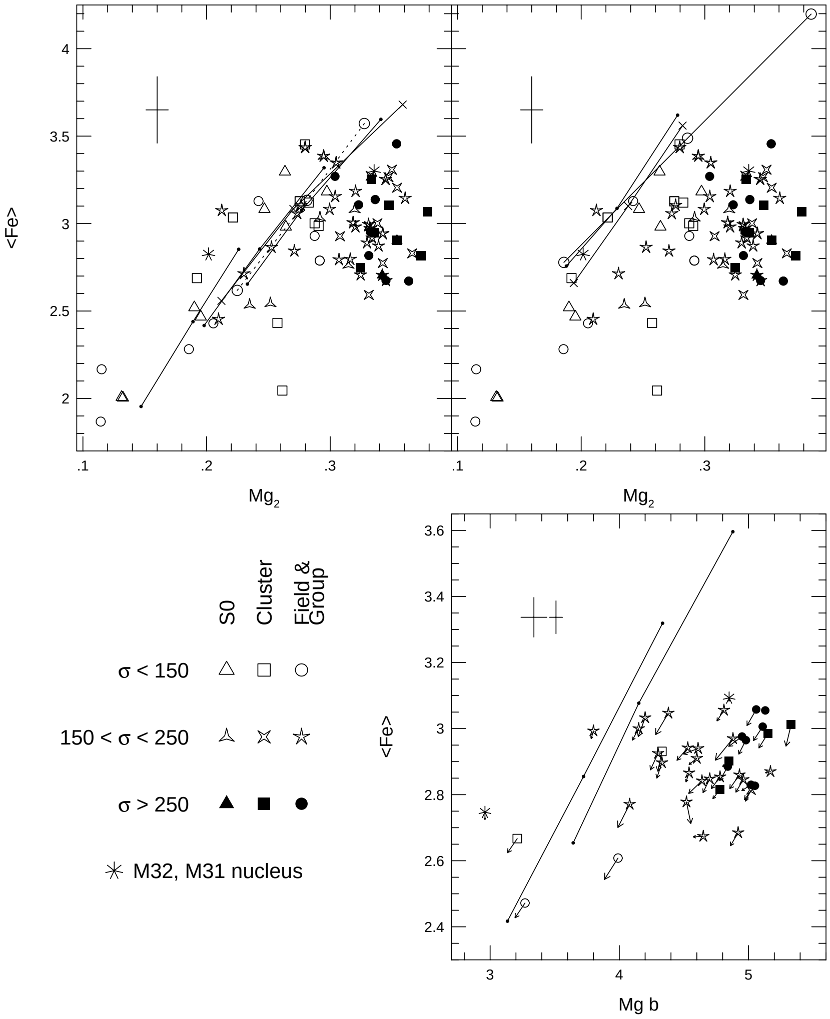

Fig. 1.— The index <Fe>= (Fe5270 + Fe5335)/2 is shown against Mg_2 and Mg b indices for Lick/IDS (Worthey, Faber, & Trager 1996) and González (1993) data, respectively. Galaxies are keyed to type, environment, and central velocity dispersion. M32 is weaker-lined than M31. Lines are models that span $-0.25 < [\mathrm{Fe/H}] < 0.25$. In the top left panel, lines with small black dots are from Worthey (1994) for ages 2, 9, and 18 Gyr, running from weak to strong index strength. The line marked with crosses is an old version of the 1994 models that was used in WFG, shown for 18 Gyr. The line marked with circles is a version of the 1994 models with Padova evolution instead of VandenBerg, also an 18 Gyr sequence. In the top right panel, models were interpolated from recent literature. Models by Weiss et al. (1995, with new evolution and index fitting functions; 15 Gyr; circles), Borges et al. (1995, with Padova evolution, new fitting functions; 16 Gyr; crosses) (16 Gyr age), and Bressan et al. (1996, with Padova evolution, Worthey et al. (1994) fitting functions; 15 Gyr; small dots) are shown. The lower panel shows gradient data from González (1993) where simulated apertures of $R_e/8$ and $R_e/2$ are shown as the symbols and arrowheads, respectively. Worthey (1994) 9 and 18 Gyr models are shown.

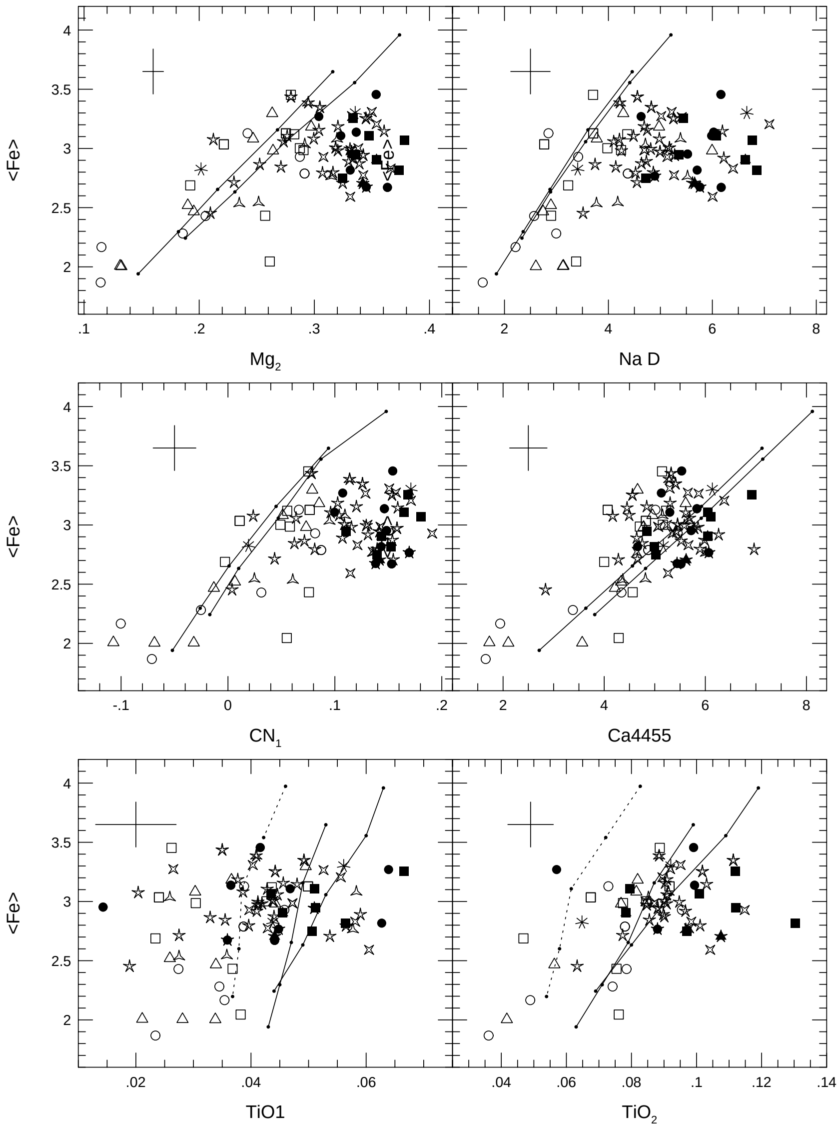

Fig. 2.— The <Fe> index is shown versus indices that measure lighter elements. Symbols are the same as in Fig. 1. Worthey (1994) models of ages 5 and 17 Gyr, and metallicities between −0.5 and +0.5 with dots marking each 0.25 dex interval are shown. Large Es clearly have enhanced Na D and CN band strengths, while Ca4455 appears nearly normal. Na D is affected by interstellar absorption upscatter, but this effect is less than 1 Å, on average. Since galaxies highest in CN are not also high in CH or C_2 index measurements (not shown), the CN enhancement is being driven by N enhancement. In the bottom panels involving TiO, an additional model sequence (dotted) shows Worthey (1994) models with Padova isochrones underneath for age 17 Gyr. The [Fe/H] = +0.5 model is an extrapolation. The large difference between the two model flavors is due to modest temperature differences for stars on the upper red giant branch, and illustrates the difficulty in modeling TiO strength due to its sensitivity to the number and temperatures of upper RGB and AGB stars.

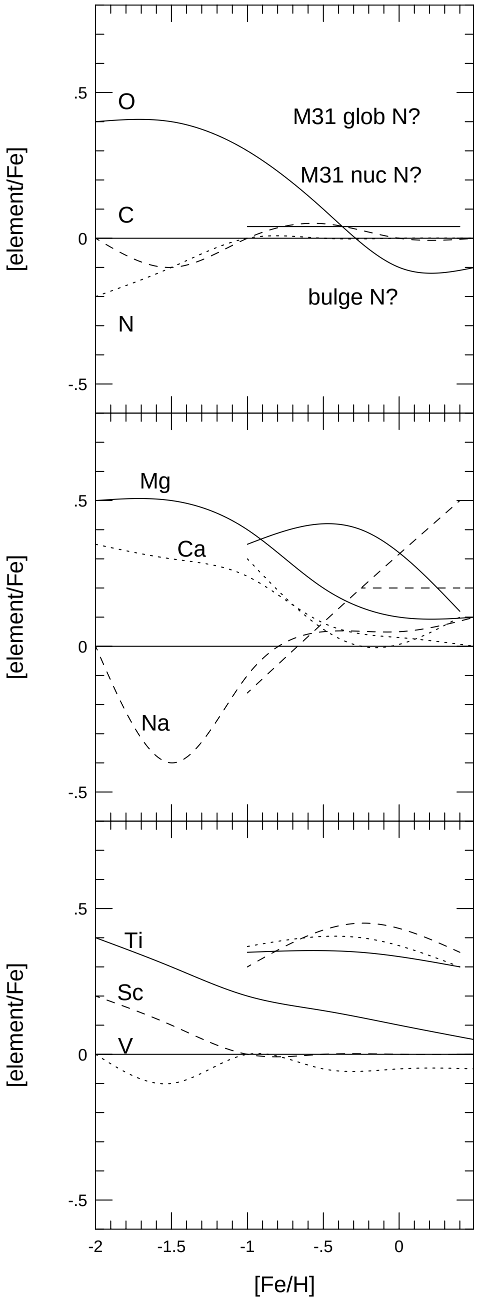

Fig. 3.— Average logarithmic abundance ratios are illustrated for disk and halo (lines that extend from [Fe/H]=–2 to +0.5) and for the bulge (lines that extend from [Fe/H]=–1 to +0.4). Average trends are distilled from stellar abundance data reproduced in Timmes, Woosley, & Weaver (1995) for the halo and disk, and McWilliam & Rich (1994) for the bulge. Bulge [O/Fe] is near zero. The high bulge [Na/Fe] value at [Fe/H]=0.4 is based on one star, so we include an alternate dashed line which stays constant at +0.2.

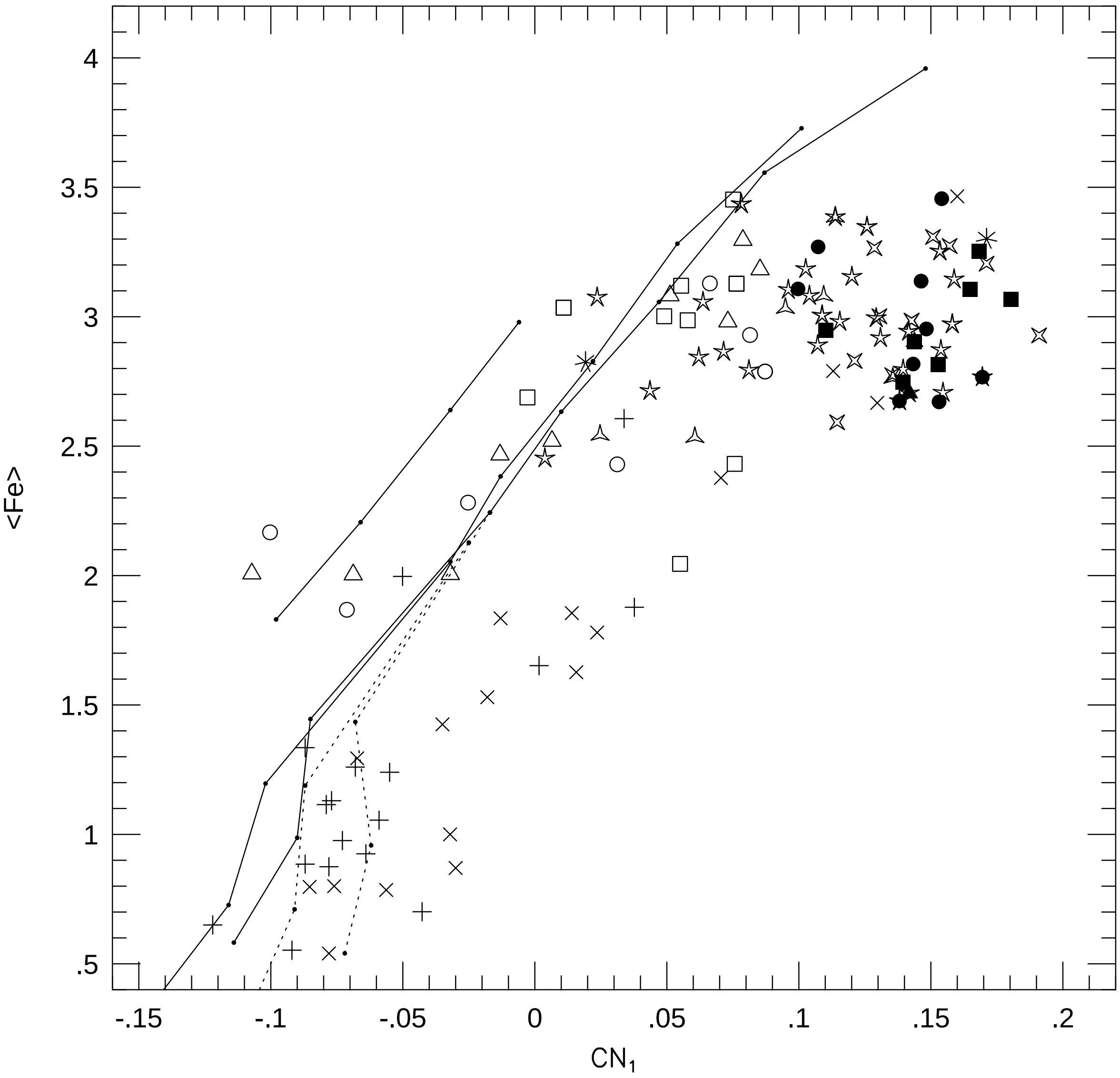

Fig. 4.— CN and Fe indices are shown for galaxies (symbols as in Fig. 1), Galactic (plus signs) and M31 (crosses) globular clusters, and models. Models are for ages 17 and 8 Gyr, with dots at [Fe/H] = −2, −1.5, −1.0, −0.5, −0.25, 0, 0.25, and 0.5. The CN index fitting functions are not calibrated below [Fe/H] = −0.5, so two different extrapolations are shown. The CN_1 index is also sensitive to the morphology of the horizontal branch. An additional model sequence is shown for age 1.5 Gyr, and [Fe/H] between −0.25 and +0.5 dex. This diagram is mildly age sensitive, but the amplitude of the age effect is not sufficient to explain the horizontal excursions of the observed stellar populations. The four leftmost galaxies appear very young in age diagnostic Balmer-metal diagrams (see Fig. 5). As for Mg, large Es have anomalously strong CN bands and therefore enhanced N abundance compared to the models and to smaller galaxies. The globular cluster sequence extends to very high metallicity when M31 clusters are included, and runs almost parallel to the reliable portion of the model sequence, but at a strongly enhanced CN strength. The nucleus of M31 competes with the largest Es in CN strength.

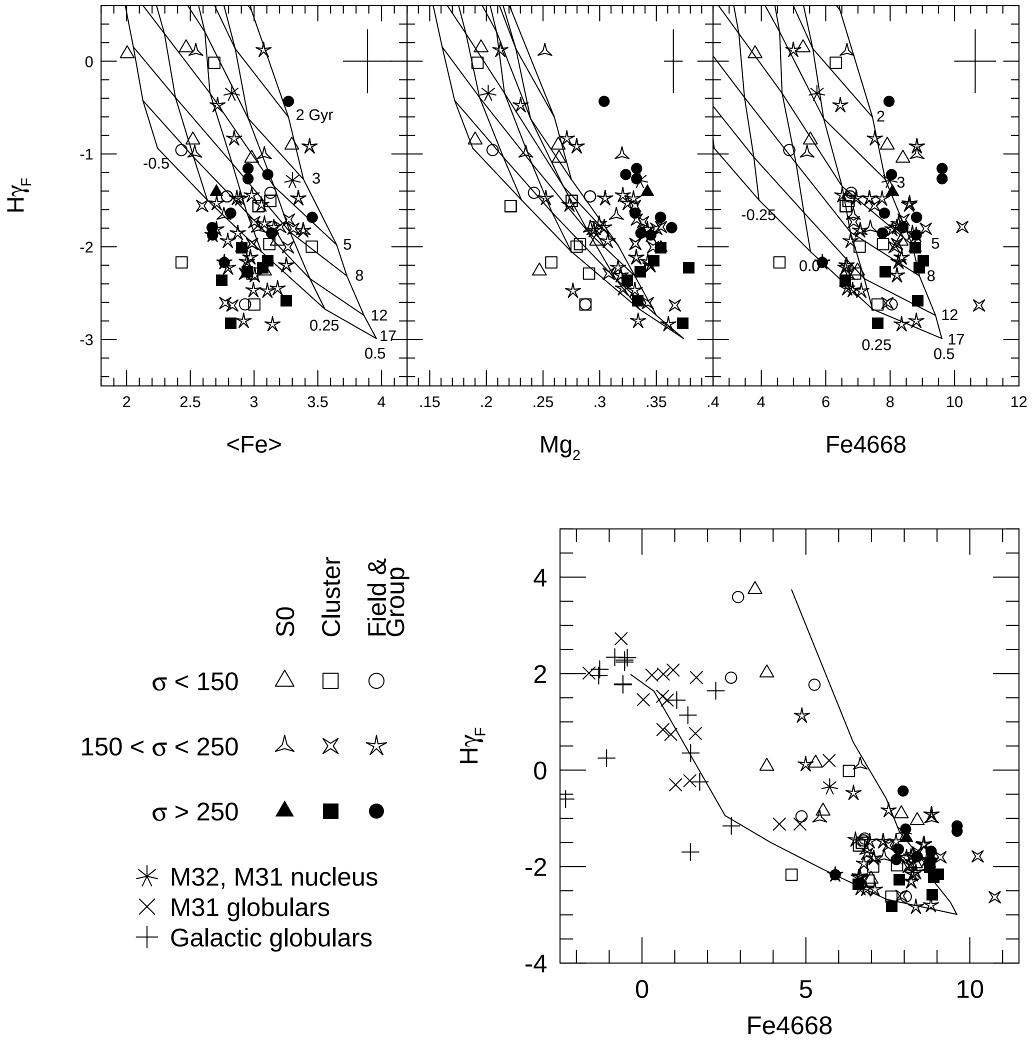

Fig. 5.— The index $H\gamma_F$ is shown versus <Fe> (the arithmetic average of Fe5270 and Fe5335), Mg_2, and Fe4668. Lick/IDS data and Worthey (1994) models are plotted. Model ages and [Fe/H] values are marked. Symbols are as in Fig. 1. Notice that the median galaxy age shifts from metal-feature to metal-feature. In the lower panel, Galactic and M31 globular clusters are also shown along with an abbreviated model sequence (17 Gyr models with $-1.5<$[Fe/H]<0.5 and +0.5 models with ages between 0.8 and 17 Gyr) in order to illustrate the strong empirical separation of the galaxian sequence and the cluster sequence. The six galaxies with the strongest $H\gamma_F$ index that appear in this diagram are off scale in the upper panels. The models strongly suggest that the galaxy sequence is primarily caused by age differences, and the cluster sequence is primarily caused by metallicity differences.

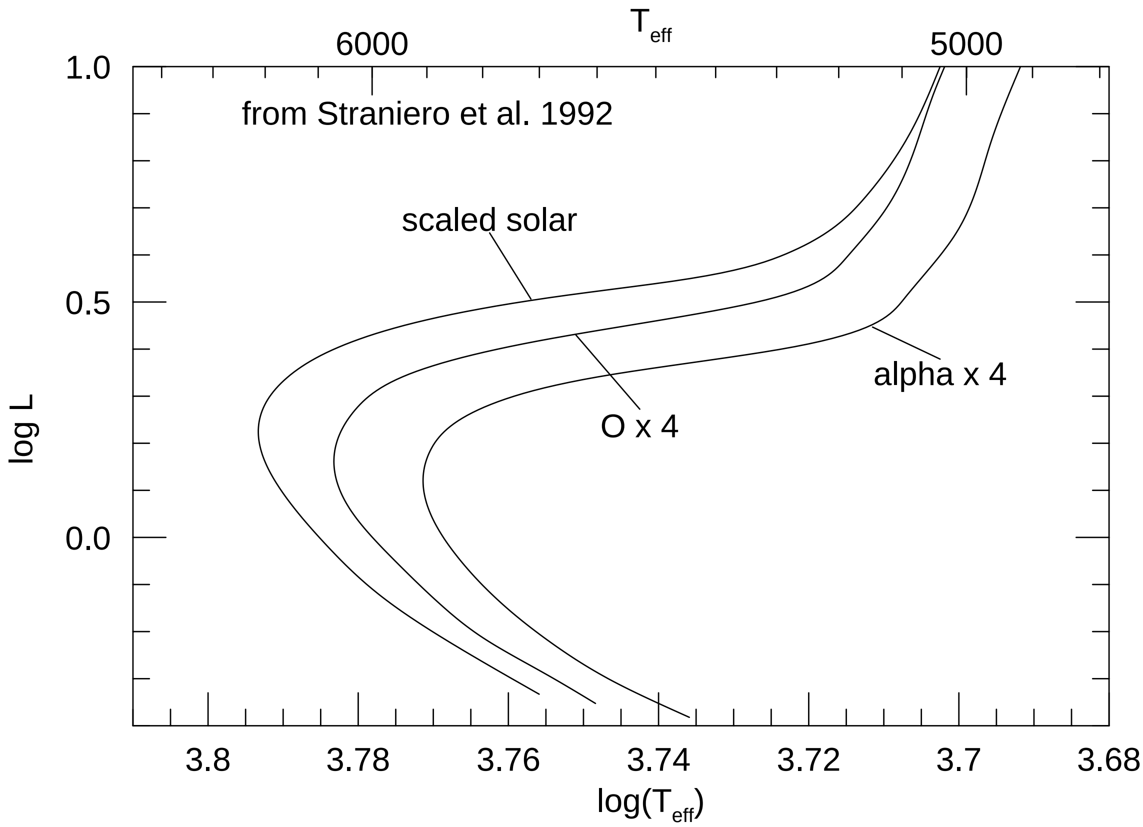

Fig. 6.— Tracks from Straniero et al. (1992) illustrating the effect that changing element ratios has on isochrone temperature. In particular, adding oxygen lowers the turnoff temperature by about 150 K, leaving the RGB unchanged. As discussed in the text, the tolerance for relative temperature changes as a function of age, metallicity, or abundance ratio is on the order of 7 K if 5% accuracy in age estimates is desired.